Analysis of 3D Printed Prosthetics Using XRD & SEM Techniques

submitted to
Professor W. Bowman
Jenna Wardini

by
Kelsey Lawson

June 10, 2020

Abstract: Within the last decade, advancements towards producing more accurate prosthetics for all ages is aided by the increasing technology of additive manufacturing, also known as 3D printing. 3D printing offers a cheaper and more customized solution to those who need prosthetics, such as children who grow out of their prosthetics. However, 3D printing involves melting plastics that cool rapidly and therefore require specific conditions to provide proper turnout. If the plastic form is pulled the wrong way it can break and if the temperature of extrusion is not regulated then cracks can form. Although, if these conditions were met, there is still the possibility of surface cracks forming that cannot be seen by human eyes. Even further, research regarding reinforcing the extruded material by blending various types of polymers to create new composites is discussed. Both, surface cracks and reinforcement, is tested by creating the material then the surface is analyzed through x-ray diffraction (XRD) or scanning electron microscopy (SEM) techniques.

INTRODUCTION

The material under investigation is 3D printed plastics that are used to create prosthetics. The ability to have any prosthetic customized to exact measurements of each patient has become very sought after. Furthermore, the plastics used, usually acrylonitrile butadiene styrene (ABS) or polylactic acid (PLA) filaments, are low cost which allows for more forgivable errors during processing [1] [2]. Also, a 3D printer ranges in the price and size for average consumer use to industrial factory use. Because the vast range of target consumers extends outside businesses, a technician isn't required to use the machines. This allows the production of products to be faster, from hours to days depending on the size of the print, instead of outsourcing a manufacturer for a supply that takes weeks to produce then deliver the said product [2].

However, due to the process of heating then extruding plastics, the amount of force that these plastic prosthetics can hold is limited when compared to traditional components with metal [4]. Those who need prosthetics normally need to replace a limb that was lost and both the arms and legs need to withstand a lot of changing stresses over a period of time. Moreover, depending on the method used for 3D printing, the layers of plastic formed may have different directions so that when a compressional or tensile load is applied the stress and strain values vary. If the shear strength is normal to the axial direction of the applied load instead of in between the layers of material, then the part will fail [4]. Further, the amount of heat applied to the plastic can negatively affect the mechanical properties which affect the range of motion that should be performed [3]. From this, the challenge of increasing the strength of plastics without overcompensating the stress-strain exhibited and the manufacturing process must be met.

The requirements needed to provide a significant 3D printed prosthetic can be analyzed through scanning electron microscopy (SEM) and x-ray diffraction (XRD) to ensure its quality. The challenge stated above results in material deformations that occur at surface level. Using these techniques prior to when the material is extruded as well as after extrusion is used for comparison of how the material transformed, if applicable. With this critical information regarding the surface of the material and its compositional analysis, advancements in research to solve the challenge of increasing 3D printed plastics' strength can be performed.

BACKGROUND THEORY

X-RAY DIFFRACTION, XRD

X-ray diffraction, XRD, is a technique used for characterizing crystalline materials by identifying crystal orientations, interatomic spacing, and percent of crystallinity, to list a few uses [5]. This technique relies on an incident x-ray source targeting the sample that then releases material-specific x-ray signals (Figure 1). These signals are detected and can be graphed by the intensity of the peak vs. its position angle (Figure 2). The position angle is also known as the Bragg angle which diffracts the outgoing x-rays. If a sample has smaller interplanar spacings then the Bragg angles appear larger, or more spaced out on the x-axis. The amount of intensity at each angle is defined by its peak width and height. Both the intensity of peaks and the position where they occur in a diffraction pattern are determined by the crystal structure - the larger the crystallites the more narrow the peaks become [6]. This means that every unit cell structure has a characteristic set of diffraction peaks and can be identified based on the intensity and position formed [6]. Experimentally, the sample is put into a diffractometer which is the machine that emits the incident beam to produce x-rays. There are various models of a diffractometer that specialize in smaller sample sizes, such as thin films, solid samples, allow for a sample to be rotated, and lose samples, the sample is horizontally stationed (Figures 3 & 4).

Using this technique in regards to 3D printed plastics is useful in determining the orientation of the material's microstructure [7]. The orientation is critical to know because the plastic is being fed into a heated nozzle undergoing heat treatment. The applied heat causes thermal expansion and then immediately cools so that it contracts. When a material heats up and expands, the position of the atoms are able to move around and have less order than when the material cools, forming its crystal structure. However, when the amount of time from applied heat to cooling is limited so that the atoms don't have enough time to follow the intended crystal order, deformations occur. Analyzing the original plastic sample before extrusion and comparing it to the extruded sample using XRD can find the percent of the crystallinity of both samples. The higher the crystallinity the harder the material, however too much can cause the material to be brittle [8]. Using the data gathered by XRD can aid in finding a solution to increasing the strength of the plastic after its been extruded.

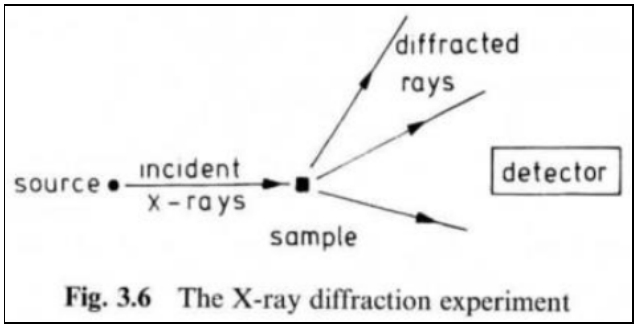

Figure 1. *Simplified diagram of a sample receiving incident beams that then produce x-rays at varying angles [6].*

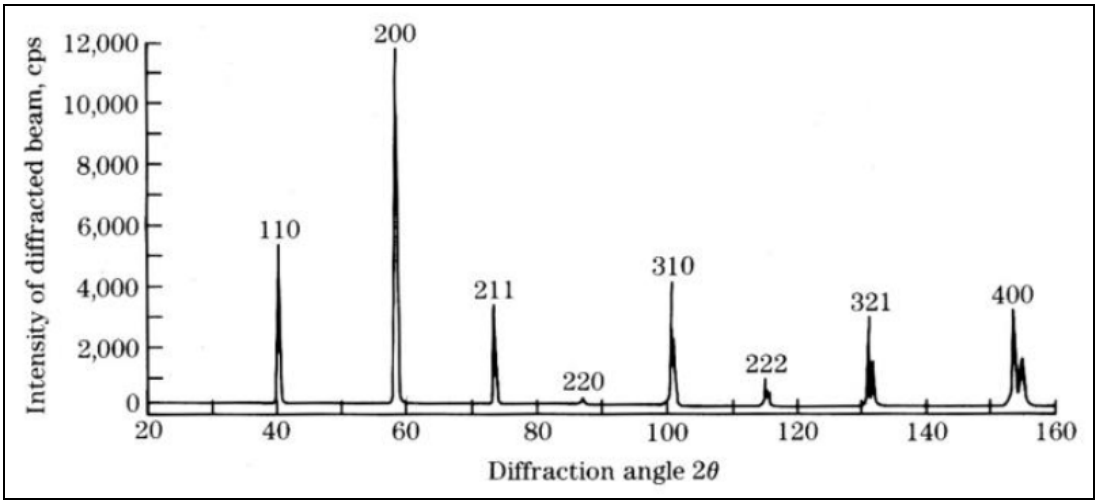

Figure 2. *A general example of what a diffraction pattern may look like. Notice that at each peak there is a defined plane in the format of (hkl). The order in which these plane values occur defines the type of lattice the material has [6].*

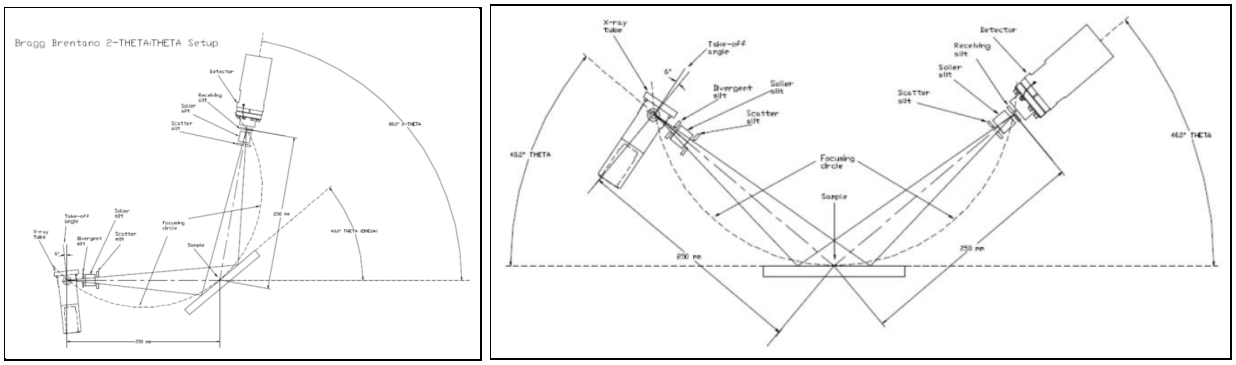

Figure 3 & 4. *On the left is an example of a diffractometer best used for solid samples. The sample stage and the detector move at an angle while the x-ray tube is stationary. On the right is an example of a diffractometer best used for powder samples. The sample stage is stationary while both the x-ray tube and detector move at an angle [6].*

SCANNING ELECTRON MICROSCOPY, SEM

Scanning electron microscopy is a technique that images the surface of a sample, usually bulk samples, through a condensed electron beam [9]. The structure of scanning electron microscopy is similar to visible-light microscopy in that a source is being condensed through lenses (Figure 5). But because electrons have a shorter wavelength than light the beam can be focused into a smaller probe, unlike light [9]. However, in SEM the beam is gradually scanning over the surface of the sample whereas in a normal optical microscope the image is lit up all at once. SEM also requires samples to be prepped before scanning if higher electrical conductivity is needed as the process occurs in a high vacuum chamber (Figure 6). Scanning electron microscopy creates its images by detecting the secondary electrons emitted by the atoms as they become excited when the beam hits [9]. The detector counts how many secondary electrons there are which is inputted as the signal intensity of the topography of the sample. There are also backscattered electrons that are produced as a result of elastic scattering. These electrons are from the incident beam making contact with the sample and then emerging back out. Their energy is dependent on the electron beam used whereas the secondary electrons have lower energy. This energy difference is reflected by the final image with backscattered electrons showing up as darker regions and secondary electrons having brighter regions (Figure 7). The magnification of SEM is not controlled like a typical microscope through the objective lenses, instead, it is a result of the supplied current to the deflector coils. These coils are controlling the direction of the beam onto the sample and the different swept areas determine the magnification.

As previously mentioned, SEM is used to determine the topography of the sample. Using this technique on 3D printed plastics will show any surface deformations that have occurred, such as fractures. Measuring the topographical image before and after the extrusion of the plastic used can give rise to any deformations that occur on the surface by the rapid temperature change. Furthermore, when a prosthetic is in use it undergoes stress - tensile or compressional stress depending on the type of prosthetic. At the beginning of a material's life, it tends to be elastic, meaning that when deformation occurs the final shape can still be recovered. However, there comes a point, the yield stress, where the shape of the material can no longer be recovered and the deformations become permanent, known as plastic deformation. The end of a material's life cycle is at the end of plastic deformation when the material finally fractures. Adjusting the composition of the material can positively extend the material's life until it fractures. With SEM, if new plastic compositions are created and tested until the surface fractures, the topography can be analyzed and compared. Knowing the fracture shape and at what load can imply assumptions of what material composition is best used to increase the strength of a prosthetic.

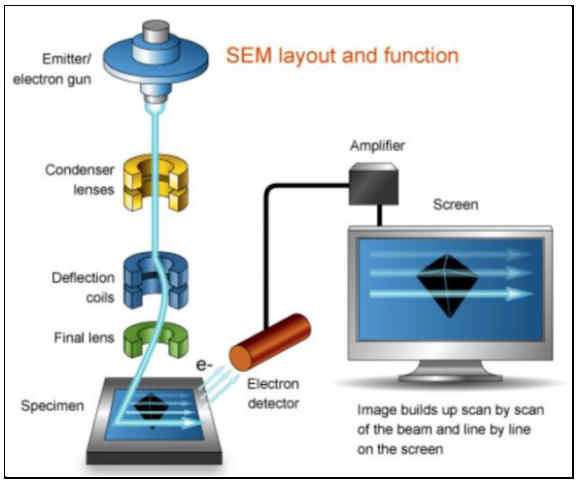

Figure 5. *The image above displays a typical layout of how SEM is processed. For SEM specifically, there is more than one condenser lens in order for a small probe [9].*

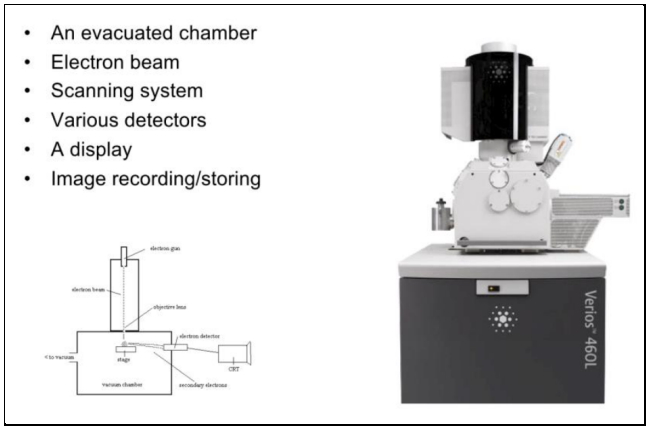

Figure 6. *This is the chamber in which all the components sit from Figure 5 [9].*

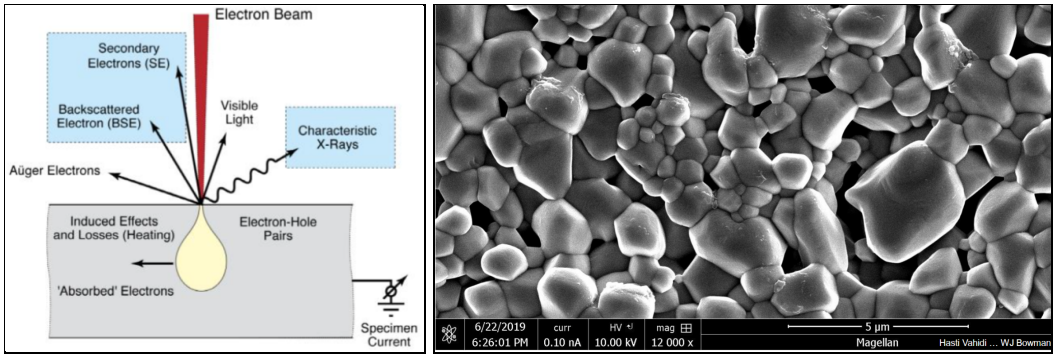

Figure 7 & 8. *The left image is a simple diagram showing how the electron beam excites the electrons creating both the secondary and backscattered electrons. The right image is a final resulting image from SEM [9].*

CASE STUDIES

EXPERIMENTAL CHARACTERIZATION & MICROGRAPHY OF 3D PRINTED PLA & PLA REINFORCED WITH SHORT CARBON FIBERS [10]

INTRODUCTION

This study's main focus was on the mechanical characterization of materials that were 3D printed based on fused filaments. The material types were polylactic acid (PLA) and then a carbon fiber (CF) enforced PLA. The study compared the strength of each material unidirectionally so that the mechanical properties exhibited were gathered under the same assumption of layer direction. The samples were tested up to the material failure and until surface fractures occurred if any. The samples were then observed through scanning electron microscopy, SEM. There were four sample surfaces observed that had varied printing angles and material types. When analyzed under SEM, it was assumed that the fibers aligned with the extrusion direction of the PLA but was not observed through injection molding. This experiment aligns with the challenge of if the composition of an extruded plastic can change its strength. SEM is used to look at the topographical fractures of both base PLA and reinforced PLA to determine if reinforcing the plastic yields higher resistance to stress.

EXPERIMENTAL METHODS

Each sample, PLA and PLA+CF, was produced when an open-source printer and applied onto a heat bed in order to prevent any warping from cooling too fast (Figure 9). The angle of layer formation varied from 0°, 90°, and ∓45°. The PLA+CF has resin reinforced short carbon fibers that have a 15% weight fraction. Both the PLA and PLA+CF have the same base material. A tensile machine was used to apply a load until material failure occurred then the fracture surfaces were evaluated by SEM.

RESULTS & DISCUSSION

Stress-strain curves were collected for both PLA and PLA+CF. The curves were post-processed so that the mechanical properties can be obtained (Figures 10 & 11). The results of the mechanical properties show that the PLA+CF tensile modulus and in-plane shear modulus was higher than PLA. From this, it shows that the reinforcement of CF in PLA provided an increase in stiffness whereas the PLA layer orientation had no effect. For the SEM results, only the 0° at 200x magnification will be reviewed as PLA only had that orientation and PLA+CF had that magnification (Figures 12 & 13). From PLA+CF SEM images it can be seen that the CF was dispersed in the PLA matrix oriented in the same direction as it was being printed. For PLA, the microstructure can be seen to take on triangular-shaped voids from being processed. Because the CF aligned with the printing direction, the stiffness also increased in the printing direction.

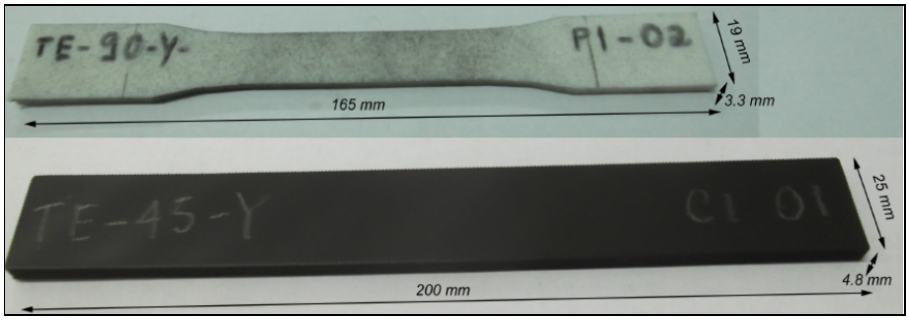

Figure 9. *The white sample is PLA and the black sample is PLA+CF. The shape of the PLA is a dog bone for tensile loading and the PLA+CF is rectangular for shear loading.*

Table 3: PLA and PLA+CF tensile and shear elastic moduli.

Property	Direction	PLA			PLA+CF			ASTM Standard
		Max.	Avg.	Dev.	Max.	Avg.	Dev.	
Tensile Modulus (MPa)	0° (E_1)	3596	3376	212	7665	7541	96	D638
	90° (E_2)	3340	3125	148	4145	3920	167	
In-plane Shear Modulus (MPa)	±45° (G_{12})	1140	1092	36	1270	1268	5	D3518

Table 4: PLA and PLA+CF Poisson coefficients.

Property	Direction	PLA			PLA+CF			ASTM Standard
		Max.	Avg.	Dev.	Max.	Avg.	Dev.	
Poisson Coefficient	ν_{12}	0.349	0.331	0.011	0.408	0.400	0.012	D638
	ν_{21}	0.336	0.325	0.014	0.163	0.150	0.008	

Table 5: PLA and PLA+CF material strengths.

Property	Direction	PLA			PLA+CF			ASTM Standard
		Max.	Avg.	Dev.	Max.	Avg.	Dev.	
Tensile Strength (MPa)	0° (S_1^*)	56.1	54.7	1.9	53.7	53.4	0.2	D638
	90° (S_2^*)	42.9	37.1	3.5	37.0	35.4	1.5	
In-plane Shear Strength (MPa)	±45° (S_{12}^*)	18.3	18.0	0.8	19.6	18.9	0.8	D3518

Figure 10 & 11. *The tables from the research paper list the mechanical properties experimentally found for both PLA & PLA+CF.*

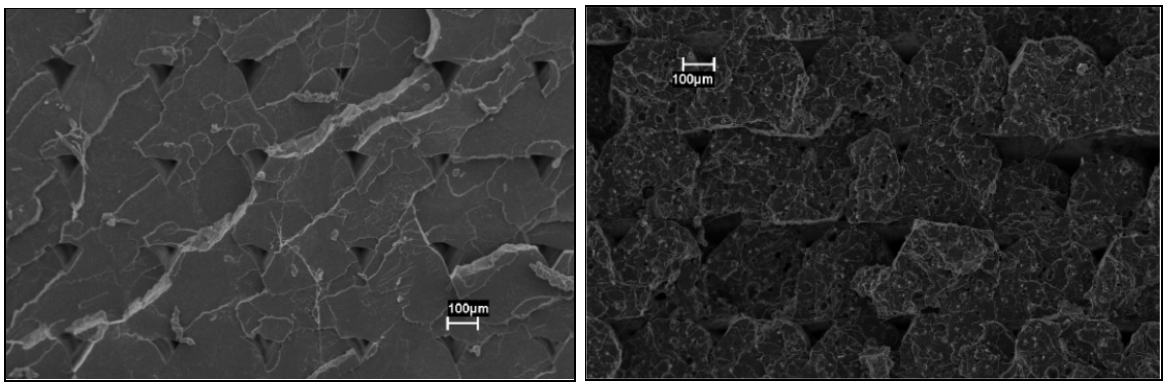

Figure 12 & 13. *The image on the left is the sample of PLA at 0° magnified to 200x. The image on the right is the sample of PLA+CF at 0° magnified to 200x.*

CHARACTERIZATION OF 3D PRINTED PLA WITH THE HELP OF MECHANICAL, DI-ELECTRIC & XRD TECHNIQUES [11]

INTRODUCTION

This study's main focus was referring to increasing the strength of #D printed materials with various manufacturing parameters. Using heterogeneous material systems they investigated the build parameters on mechanical, electrical, and crystalline properties. X-ray diffraction was used to analyze the crystallinity of 3D printed PLA at various infill parameters in order to find improvements of strength or stiffness. The average crystallinity percentage was calculated for a total of twelve runs sub grouped into four categories of pattern types of infill. The linear and diamond infill patterns showed a decrease of crystallinity percentage when they were at 100% infill and observed a low elongation break. This experiment aligns with the challenge presented regarding the strength of the material being found through XRD. Knowing the percentage of crystallinity in the printed plastic material can determine at what percentage should be applied for maximum strength without making the prosthetic too brittle that it fails faster.

EXPERIMENTAL METHODS

The samples were printed with regards to fused deposition modeling - the plastic is extruded as the nozzle moves around the plate and the plate is also heated. For the XRD analysis, the Siemens XRD D500 machine was used alongside a peak fitting software that calculated the crystallinity percentage. The 3D printed samples were a 1x1" square and the Cu-Kα radiation was used with the scan settings (Figure 14).

RESULTS & DISCUSSION

The crystallinity was calculated from three different runs for the top and bottom of the samples and the average of the percentages is considered. From the graphed average crystallinity it can be observed that the Linear and Diamond Infill shape had decreased once it hit 100% infill. However, the Hexagonal Infill at 100% infill was able to maintain an increase in crystallinity percentage. Reviewing the rest of the infill percentages, a trend could be seen where each specimen exhibited an increase in crystallinity (Figures 15 & 16). It can be assumed that the lower crystallinity percentages when at 100% infill is because there are little to no gaps in the samples. Without gaps, it prevents the crystal from growing and can lead to internal stresses affecting the ultimate tensile strength of each sample.

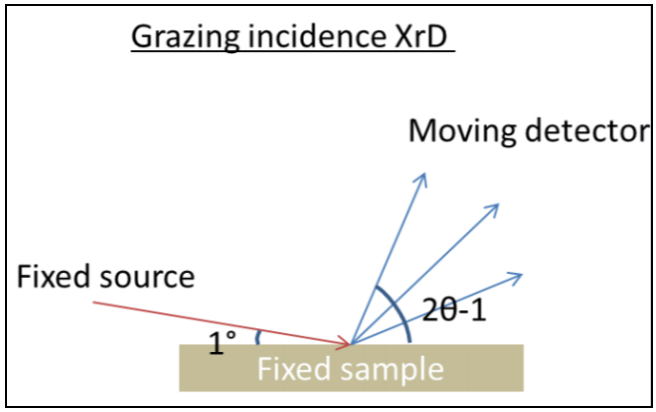

Figure 14. *The XRD incidence on the sample is shown.*

Infill%	Pattern	Bottom	Top	Avg Crystallinity%
25	linear	19.031	18.5221	18.77653209
50	linear	16.5152	22.5942	19.55471903
75	linear	22.0667	18.3025	20.18461788
100	linear	17.0715	17.7821	17.42683101
25	diamond	17.0548	18.9117	17.9832488
50	diamond	20.5572	20.4749	20.51601297
75	diamond	20.5718	20.8347	20.70326567
100	diamond	21.882	22.9163	22.39913676
25	hex	17.7848	20.1761	18.98043407
50	hex	19.9948	20.9414	20.46809986
75	hex	22.013	22.2698	22.14137952
100	hex	24.234	22.4167	23.32538172

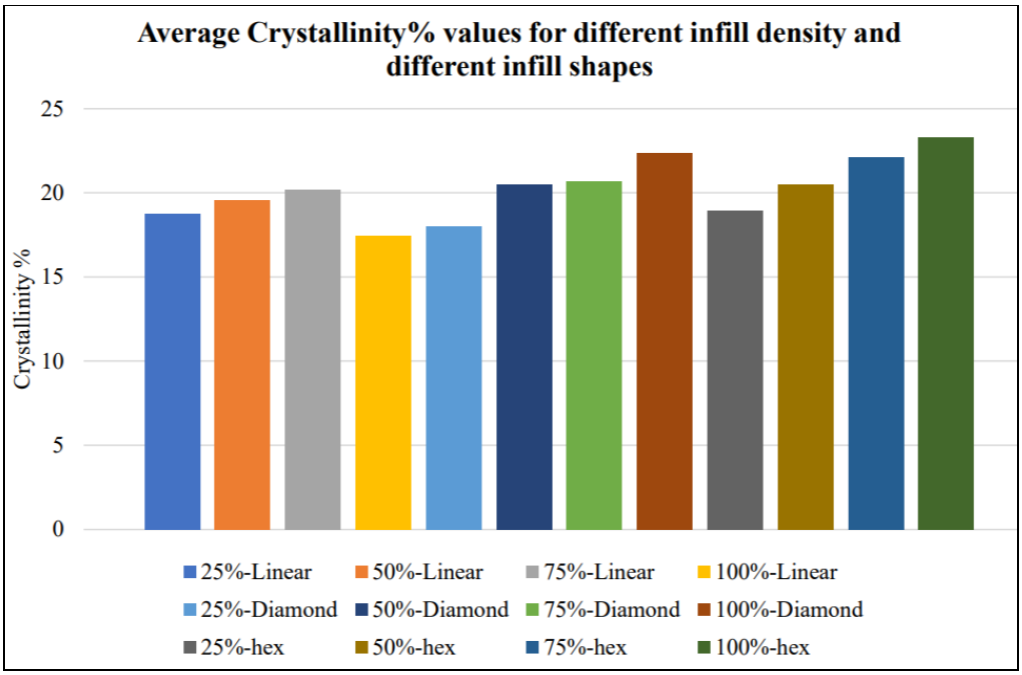

Figure 15 & 16. *The top image shows the average crystallinity percentage is shown for each set. The bottom image is the values from the table graphed.*

FRACTURE SURFACE ANALYSIS OF 3D PRINTED TENSILE SPECIMENS OF NOVEL ABS-BASED MATERIALS [12]

INTRODUCTION

This study's main focus was looking at the effect of adding reinforcement to acrylonitrile butadiene styrene (ABS) for improved mechanical properties to produce enhanced physical properties. They compared pure ABS as well as two ABS composites, and an elastomer ABS blend. Analyzing each material for the fracture surface was done by using scanning electron microscopy, SEM. Depending on the additives, a specific mode of failure could be traced back to how pure ABS was transformed. Each sample showed dramatically different results of behavior from the expectation of seeing characteristics for ductile fractures. Additives to ABS resulted in fracture surfaces similar to brittle but higher ultimate tensile strength, UTS, than pure ABS. This experiment aligns with the challenge of if the composition of an extruded plastic can change its strength. SEM is used to look at the topographical fractures of both base ABS and compositionally altered ABS to determine if the composition changes the maximum stress before fracture.

EXPERIMENTAL METHODS

ABS was used as the matrix material while it was loaded with: 5 wt.% jute fiber or 5 wt.% TiO2 and then for the polymeric blend, ABS was mixed with 5 wt. % of a TPE (Figure 17). The printing method was extrusion and the three ABS-based materials were compared with the ABS filament. These samples had SEM imaging before the additives were added and processed. There are two sets of each sample with one being printed in the XYZ direction and the other being printed in the ZXY direction (Figure 18). The samples are put under tensile stress & will have the fracture surfaces observed through SEM.

RESULTS & DISCUSSION

All samples, for each printing direction, had fractured in the gage section of the tensile machine. Adding the reinforcements to ABS affected the mechanical properties and fracture surface characteristics compared to base ABS. However, the additives did not improve on ABS naturally ductile properties, instead the sample exhibited brittle characteristics. But, the additive samples had a much higher ultimate tensile strength than pure ABS but resulted in a shorter strain range that contributed to the brittleness. In the ZXY printed sample direction, there were cavities resulting from a failure of the interface between the printed layers (Figures 20 & 21). This means the mechanical strength of parts printed in the direction is considerably lower than in the XYZ.

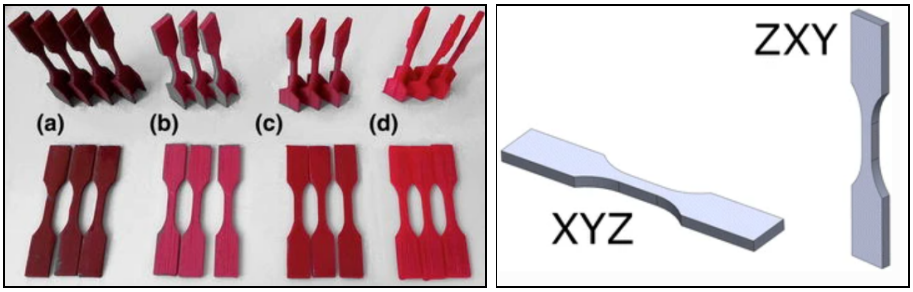

Figure 17 & 18. *The left image is the sample types: (a) ABS & jute fiber, (b) ABS & TiO2, (c) ABS with TPE, and (d) pure ABS. The right image is the printing direction. The nozzle of the 3D printer would be directly above the sample plate.*

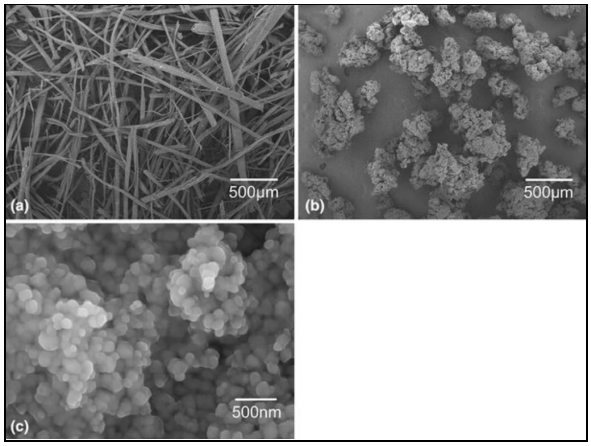

Figure 19. *The SEM images of the additives before being added to the ABS matrix: (a) jute fibers, (b) TPE, (c) TiO2.*

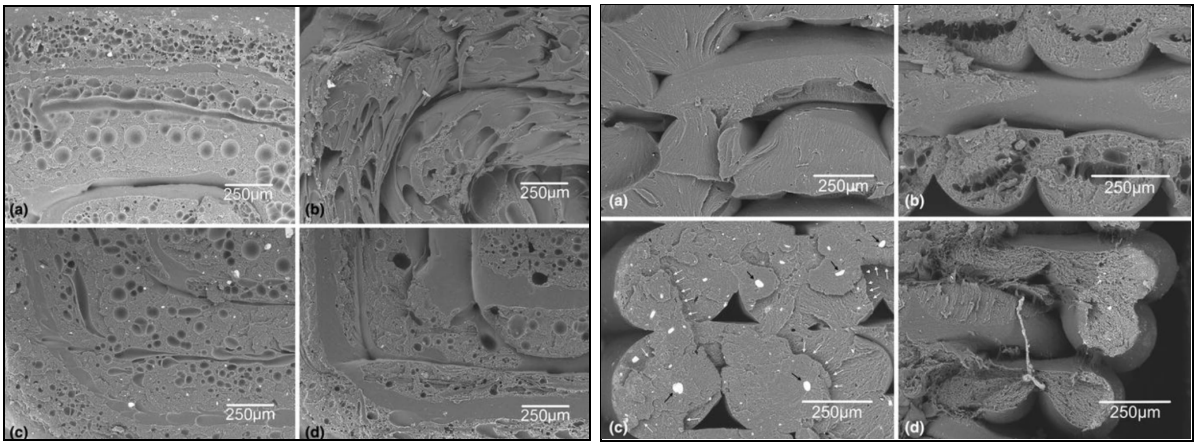

Figure 20 & 21. *The image on the left are the SEM images of the fractures in the ZXY direction at low magnification. The image on the right are the SEM images of the fractures in the XYZ direction at low magnification. The samples in both images are listed as: (a) ABS, (b) ABS & jute fiber, (c) ABS & TiO2, and (d) ABS & TPE.*

CONCLUSION & FUTURE WORK

From the mentioned case studies, each looked into increasing the strength of 3D printed plastics either through different material compositions or increasing crystallinity through infill percentage. These address the issue of 3D printed objects and how much force can be applied before fracturing, or shattering. Analysis through scanning electron microscopy (SEM) or x-ray diffraction (XRD) was used to provide more insight into the material's microstructure and how it affected the overall quality.

For case studies 1 & 3, both tested the mechanical properties of plastics with additives and used SEM to analyze the fracture point under tensile loading. From each experiment, it seemed that improving the base plastic matrix is heavily dependent on the type of additive added. In the first case, an improvement in stiffness due to the carbon fibers added was seen. However, relating it back to prosthetic making, the difference from the base PLA results and the PLA+CF wasn't all that drastic. In the end, extending the length of carbon fibers to the PLA matrix should be researched further and may have better benefits of adding something to PLA for prosthetics. On the contrary, the last case's experiment had experienced no beneficial increase in stiffness, but rather the worst case in creating a brittle material. For prosthetics, this material type is not desirable because of how short the overall time is before the material fails under the applied stress. A new study comparing PLA and ABS both having carbon fiber additives would be interesting and pose the question of what common 3D printed plastic is more useful for prosthetics.

For the second case study, the focus was on how layering the printed material can increase strength or stiffness and used XRD to determine the amount of crystallinity present at each infill percentage and shape. This experiment, unlike the two others, dealt with the amount of material being printed at a time. This led to some interesting results showing that the hexagonal infill shape showed an increase in crystallinity, or hardness, as the infill percentage increased. Although the material will get harder with maximum infill as a hexagonal shape, for prosthetics, allowing for some flexibility through minimizing the infill may be better. Too hard of a prosthetic would increase the volume, and therefore the density. Too heavy of a prosthetic could result in discomfort to the patient even though the prosthetic may last longer.

Expanding on 3D printed prosthetics, looking into the research of additive manufacturing of metals or ceramics would extend the possibilities of mechanical properties because these materials differ from the traditional thermoplastics used. Also, narrowing the research to a specific type of prosthetic would allow for more refined conclusions of what should be expected by the material properties.

REFERENCES

[12] Berman, B., et al. “Fracture Surface Analysis of 3D-Printed Tensile Specimens of Novel ABS-Based Materials.” Journal of Failure Analysis and Prevention, Springer US, 20 Mar. 2014, link.springer.com/article/10.1007/s11668-014-9803-9.

[6] Bowman, William J. “Lecture 4: General Principles of XRD & Braggs’ Law.” MSE 164, April 2020, University of Califonia, Irvine. PDF.

[9] Bowman, William J. “Lecture 12: Introduction to (scanning) Electron Microscopy & SEM Operating Principles.” MSE 164, April 2020, University of Califonia, Irvine. PDF.

[10] “Experimental Characterization and Micrography of 3D Printed PLA and PLA Reinforced with Short Carbon Fibers.” ResearchGate, www.researchgate.net/publication/316897831_Experimental_characterization_and_micrography_of_3D_printed_PLA_and_PLA_reinforced_with_short_carbon_fibers.

[4] Gordon, Matt, et.al. “3D Printed Dexterous Prosthetic Foor Structure Design.” *The University of Southern Maine.* 2016. PDF.

[3] Gretsch, Kendall F, et al. “Development of Novel 3D-Printed Robotic Prosthetic for Transradial Amputees - Kendall F Gretsch, Henry D Lather, Kranti V Peddada, Corey R Deeken, Lindley B Wall, Charles A Goldfarb, 2016.” *SAGE Journals*, journals.sagepub.com/doi/full/10.1177/0309364615579317.

[1] Manero, Albert, et al. *Implementation of 3D Printing Technology in the Field of Prosthetics: Past, Present, and Future*. 10 May 2019, www.ncbi.nlm.nih.gov/pmc/articles/PMC6540178/.

[11] Munaganuru, Sai. “Characterization of 3D Printed PLA with the Help of Mechanical, Di-electric, and X-Ray Diffraction techniques.” *The University of Texas at Arlington.* May 2019. PDF.

[8] Oxford dictionary of science, 1999, ISBN 0-19-280098-1

[7] “Use of X-Ray Diffraction Analysis to Determine the Orientation of Single-Crystal Materials.” American Laboratory, www.americanlaboratory.com/914-Application-Notes/1593-Use-of-X-ray-Diffraction-Analysis-to-Determine-the-Orientation-of-Single-Crystal-Materials/.

[2] Ventola, C Lee. “Medical Applications for 3D Printing: Current and Projected Uses.” *P & T : a Peer-Reviewed Journal for Formulary Management*, MediMedia USA, Inc., Oct. 2014, www.ncbi.nlm.nih.gov/pmc/articles/PMC4189697/.

[5] “X-Ray Diffraction: Instrumentation and Applications.” *Taylor & Francis*, www.tandfonline.com/doi/abs/10.1080/10408347.2014.949616.